PROBABILITY OF COLLISION IN THE GEOSTATIONARY ORBIT*

Raymond A. LeClair and Ramaswamy Sridharan

MIT Lincoln Laboratory, 244 Wood Street, Lexington, Massachusetts 02420 USA, Email: Sridharan@ll.mit.edu

ABSTRACT/RESUME

The advent of geostationary satellite communication 37 years ago, and the resulting continued launch activity, has created a population of active and inactive geosynchronous satellites which will interact, with genuine possibility of collision, for the foreseeable future. As a result of the failure of Telstar 401 three years ago, MIT Lincoln Laboratory, in cooperation with commercial partners, began an investigation into this situation. Under the agreement, Lincoln worked to ensure a collision did not occur between Telstar 401 and partner satellites and to understand the scope and nature of the problem. The results of this cooperative activity and recent results to carefully characterize the actual probability of collision in the geostationary orbit are described.

1. INTRODUCTION

On 11 January 1997 Telstar 401 failed on-orbit in the geostationary belt. It will now oscillate indefinitely near the geopotential well at 105 degrees West longitude, next year passing within ten to thirty kilometers of twenty-two active satellites stationed between 97 and 113 degrees West longitude. The behavior of Telstar 401, typical of inactive geosynchronous satellites, led six commercial satellite operators (AMSC, DirecTV, GE Americom, PanAmSat, SATMEX and Telesat Canada) to enter into a Cooperative Research and Development Agreement (CRDA) with MIT Lincoln Laboratory. The resulting cooperative activities sought to assess and respond to the threat posed by Telstar 401. With over 40 years of space surveillance technology development and sensor operations, MIT Lincoln Laboratory was recognized to be uniquely positioned to properly address this geosynchronous encounter threat. The longitude oscillation of Telstar 401 and resulting encounters with active satellites are shown in Fig. 1.

The initial Geosynchronous Encounter Analysis (GEA) CRDA spanned two years beginning in mid 1997. During this period, Lincoln Laboratory provided timely warning of encounters between Telstar 401 and partner satellites and precision orbits for these objects for use in avoidance maneuver planning [1]. In all, 32 encounters between Telstar 401 and a partner satellite were supported in 24 months leading to nine avoidance maneuvers incorporated into routine station keeping and six dedicated avoidance maneuvers. This process has led to a validated concept of operations for encounter support at Lincoln.

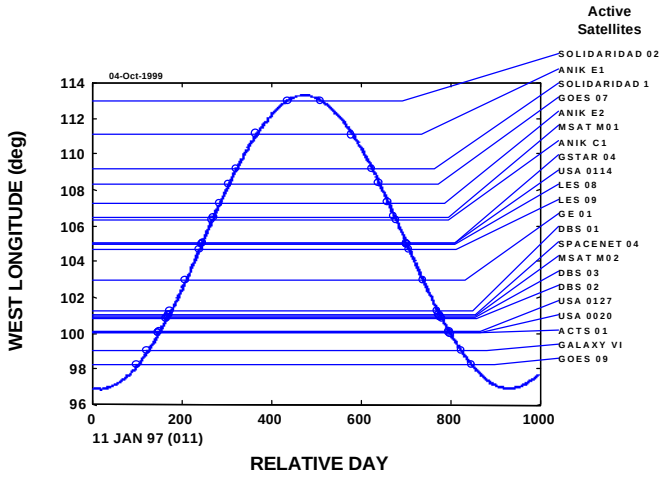

Fig. 1. Telstar 401 Encounter Situation

In addition, as part of the cooperative agreement, a number of important research objectives were accomplished. Abbot and Thornton [2] undertook calibration of partner satellite ranging data to establish procedures for routine receipt, calibration and processing of partner ranging data for use in precision orbit determination. Abbot and Sharma [3] investigated the optimum mix of sensor data needed to meet orbit accuracy requirements for encounter support, finding that a combination of radar and optical data synergistically produces precision orbits with relatively few observations.

*This work was performed under a cooperative Research and Development Agreement (CRDA 922) between MIT Lincoln Laboratory and PanAmSat. Opinions, interpretations, conclusions, and recommendations are those of the authors and do not necessarily represent the view of the U.S. Government.

Recently, in late August 00, another satellite failed in orbit in the same region of the geosynchronous orbit. Solidaridad 1 is a SATMEX satellite that was located at 109° W sublongitude in the path of Telstar 401. From being threatened, it has now turned into a threat itself. Its predicted longitude drift is between 101° W. and 109° W thus overlapping a part of the path of Telstar 401. In addition, there was significant concern raised by Galaxy 7, owned by Panamsat, when it also failed in situ at 125° W sublongitude in late November 00. However, Boeing and Panamsat were successful in regaining control and boosting it out of geosynchronous orbit. These incidents illustrate that unexpected failure of large satellites in GEO may well continue to happen.

In order to determine the magnitude of the geosynchronous encounter threat, we determined the number of encounters between all active (approximately 270) and inactive geosynchronous objects (approximately 430). An encounter was defined as a difference in geocentric radius less than 200 km and in longitude less than 0.2 degrees at the locations of the orbital plane intersections. Active satellites were considered to reside at the center of their station-keeping box given by the semi-major axis and longitude of the ascending node of their orbit. Inactive satellites that could approach the geostationary radius (42,166 km) within 200 km were propagated from August 1998 to August 1999 using DYNAMO, a precision numerical propagator developed at MIT Lincoln Laboratory and discussed more fully below. The resulting distribution of encounters as a function of the distance of closest approach is shown in Fig. 2. Considering only those encounters with a distance of closest approach not more than 50 km, the results indicate 4152 encounters, between an active, geostationary satellite and an inactive, geosynchronous object, will occur annually.

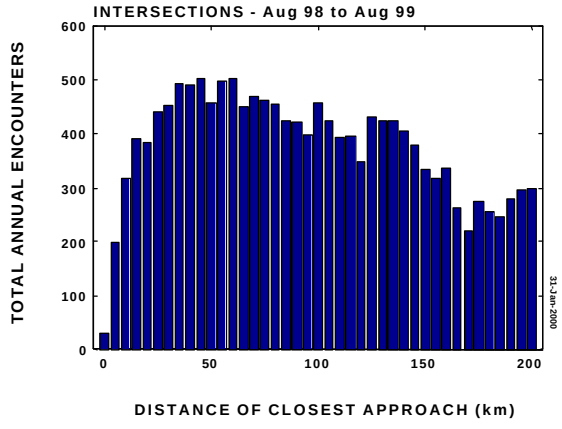

Fig. 2. Distribution of Encounter Distance of Closest Approach

Although it was the failure of Telstar 401 and the resulting activity at Lincoln Laboratory which led to the recognition of this geosynchronous encounter problem, the situation arises as an unavoidable consequence of the recent launch history of geostationary communication satellites. The first successful geostationary communication satellite, Syncom II, launched in 1963 inaugurated a flurry of geostationary launch activity which gave rise to the initially rapid but continuing increase in the geostationary satellite population shown in Fig. 3, using data from the Lincoln Space Surveillance Center (LSSC) databases. Initially this launch activity was dominated by military launch activity but during the mid 1980s to mid 1990s commercial launch activity began to dominate.

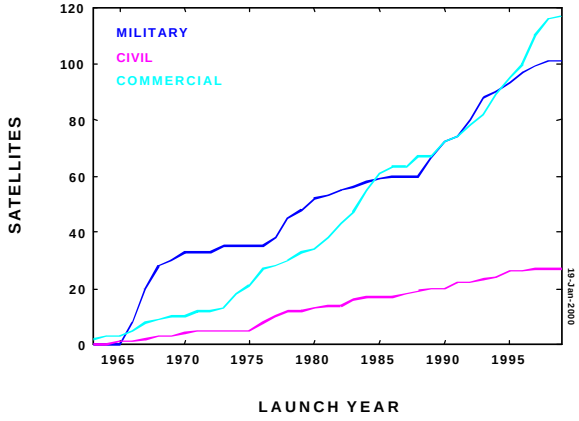

Fig. 3. Thirty Years of Cumulative Launch Activity

As a result of the encounter support concept of operations developed and validated at MIT Lincoln Laboratory and the accompanying investigation into the scope and nature of the problem, the initial two year CRDA has been extended for an additional two years. As part of the continued CRDA activity, Lincoln Laboratory will develop a system to monitor encounters between all cataloged, inactive threatening resident space objects and GEA CRDA partner satellites. Objectives of the system include automation of encounter support to produce the highest quality orbits and fewest false alarms while minimizing sensor time and analyst involvement. A conceptual block diagram of the Geosynchronous Monitoring and Warning System (GMWS) is shown in Fig. 4.

In addition to the development of the GMWS, Lincoln has taken a careful look at the probability of collision in the geostationary orbit, the description of which forms the purpose of this document.

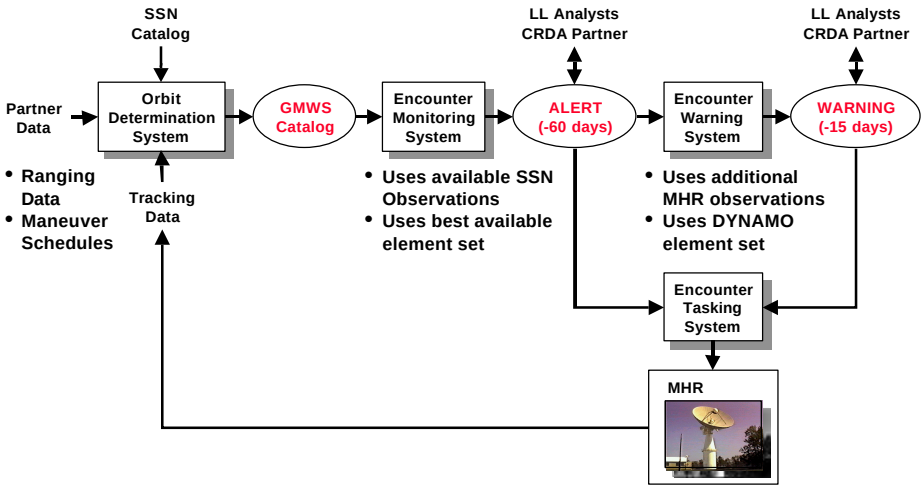

Fig. 4. Geosynchronous Encounter Monitoring and Warning System Concept

2. PROBABILITY OF COLLISION

Several authors have considered the problem of on-orbit collisions. For geostationary satellites, Hechler and Van der Ha [4] consider the probability of collision for the population of geostationary satellites on-orbit in 1981 and determine an annual collision rate of 6×10^{-6}. In the same year, Kessler [5] presents a straightforward approach, which may be used to estimate the collision probability between orbiting objects in general. Kessler's approach is adapted and discussed below. Much more recently, a number of authors, including Alfriend [6] (and others) and Chan [7], have considered the probability of an on-orbit collision using the orbital covariances. The work by Chan, funded as part of the Iridium program by Motorola, is representative of this approach and is also discussed below.

2.1 Probability of Collision Based on Orbital Covariances

By noting that the covariance matrices for the two orbits under consideration may be transformed to a common coordinate system, and noting that the random variables for the two orbits are independent, Chan shows that the covariances may be combined as a sum. Then by establishing an encounter coordinate system with *xz* plane and origin defined by the expected relative velocity and separation at the point of closest approach and aligning the *x* axis with the two objects, Chan arrives at a bivariate normal distribution for the separation at the point of closest approach with joint probability density function

$$f_2(x,z) = \frac{1}{2p\,s_x s_z\sqrt{1-r_{xz}^2}}\times e^{-\left[\left(\frac{x}{s_x}\right)^2 - 2r_{xz}\left(\frac{x}{s_x}\right)\left(\frac{z}{s_z}\right)+\left(\frac{z}{s_z}\right)^2\right]\left[\frac{1}{2\left(1-r_{xz}^2\right)}\right]} \quad (1)$$

where σ_x, σ_z, and r_{xz} are the separation standard deviations and correlation coefficient. For the case in which the collision radius, r_a, is much less than σ_x and σ_z, $f_2(x,z)$ may be integrated over the collision area, to obtain the collision probability $P = \iint_A f_2(x,z)dxdz$, by using the constant value $f_2(x_e,0)$, where x_e denotes the expected value of the separation at closest approach, to obtain

$$P = \frac{r_a^2}{2s_x s_z\sqrt{1-r_{xz}^2}}\,e^{-\left[\frac{x_e^2}{2s_x^2\left(1-r_{xz}^2\right)}\right]} \quad (2)$$

Although not noted by Chan, for the case in which x_e is small relative to σ_x the probability of collision may be approximated by

$$P = \frac{r_a^2}{2s_x s_z\sqrt{1-r_{xz}^2}} \quad (3)$$

which may be interpreted as the ratio of the collision area to the area over which the satellites are uniformly distributed at the point of closest approach. Chan continues, as does Alfriend, by noting the probability of collision may be placed in the following form

$$P = \frac{1}{\sqrt{2p}\,s_x}\int_{x_e-r_a}^{x_e+r_a} e^{-\left(\frac{x^2}{2s_x^2}\right)}\times \frac{1}{2}\left[erf\left(\frac{l+m}{\sqrt{2}s'}\right)+erf\left(\frac{l-m}{\sqrt{2}s'}\right)\right]dx \qquad (4)$$

by completing the square in the z term, rearranging to make use of the error function and noting that the error function is an odd function, where

$$l = \sqrt{r_a^2-(x-x_e)^2}$$
$$m = \frac{r_{xz}s_z}{s_x}x \qquad (5)$$
$$s' = s_z\sqrt{1-r_{xz}^2}$$

and the error function is defined by

$$erf(x) = \sqrt{\frac{2}{p}}\int_0^{\sqrt{2}x} e^{-t^2/2}dt \qquad (6)$$

Eq. 4 may be integrated numerically to gain physical insight into the form of the collision probability as a function of the separation standard deviation, σ_x, relative to the expected separation at the point of closest approach, x_e, by assuming $r_{xz} = 0$ to obtain the result shown, in blue, in Fig. 5. Note that the functional form remains the same for the three ratios of x_e relative to the collision radius, r_a, shown and exhibits a maximum near $s_x/x_e = 1/\sqrt{2}$. Also shown in Fig. 5, in magenta, is the corresponding result from Eq. 2. Note that except for the case in which x_e is only slightly larger than r_a is there any appreciable difference in the result. More significantly, the probability of collision, which results using Eq. 3 differs very little from these results provided $\sigma_x > x_e$. Therefore, for values of σ_x increasingly greater than x_e the difference in probability of collision obtained by assuming a uniform rather than a bivariate normal distribution is increasingly negligible.

The interpretation of the probability of collision resulting using Eq. 4 in the region in which σ_x is smaller than x_e must be handled carefully. In this region the value of the probability of collision is increasingly determined by the tails of the separation probability density function which increasingly implies that the position of the satellites actually depart from the estimate by many standard deviations. In other words, were one to consider the satellite observations residuals one would find meaningful observations many standard deviations from the expected value. In fact, of course, such observations are routinely discarded as unphysical in the orbit determination process. Eq. 4 is not physically meaningful in the region where σ_x is much less than x_e, since all that can be said is that the probability of collision is small; little may be meaningfully said about the order of that smallness. Furthermore, where Eq. 4 is perhaps applicable it is not needed since the probability of collision may be determined as a ratio of areas using Eq. 3.

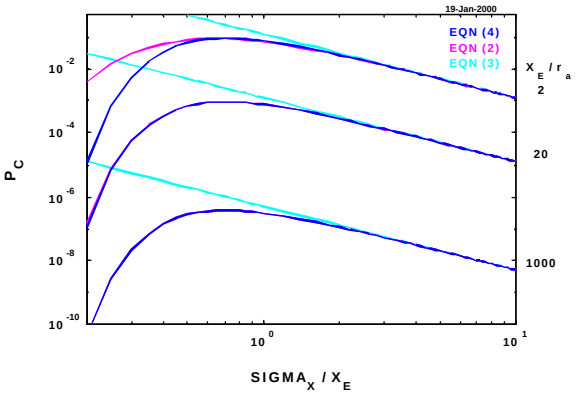

Fig. 5. Probability of Collision

Another facet of this interpretation involves the realization that the orbit standard deviation describes the estimated rather than actual, physical trajectory of the satellite. That is, the trajectory of the orbiting objects is very well behaved and does not exhibit a significant random character, although our estimate of its position does.

2.2 Probability of Collision Based on Volume Density

Consider now the probability of collision estimate which can be obtained following Kessler. Suppose N_A objects are actively maintained in a circular orbit of radius $R \pm e_r$ and inclination e_q, where e_r and e_q are constants representing the uncertainty in the orbital position. Then the volume density of these objects is

$$\frac{N_A}{2e_r(2e_qR)(2pR)} \qquad (7)$$

Suppose an object is inactive in a circular orbit of radius R and inclination i. Denote the velocity of this object by V. This object spends

$$\frac{2e_qR/(V\sin i)}{2pR/V} \qquad (8)$$

of its orbital period in the volume occupied by the active objects, provided $e_q > i$. Note that under the current circular orbit assumption, the inactive object spends

tive objects as indicated by Eq. 8. However, the eccentricity of most inactive geosynchronous objects typically limits the close approach to only one point on the intersection of the orbital planes. This reality is accounted for in Eq. 8. Suppose all of the objects are spherical and have a radius denoted by r. Denote the collision cross-sectional area by σ and assume, as an approximation, that $\sigma = 2\pi r^2$. The collision velocity is given by

$$V[(\cos i - 1)^2 + \sin^2 i]^{1/2} = V[2(1-\cos i)]^{1/2} \qquad (9)$$

Therefore the inactive object encounters volume potentially occupied by an active object at the rate

$$V[2(1-\cos i)]^{1/2} s \qquad (10)$$

As a result the collision rate is given by combining Eqs. 7, 8, and 10 to obtain

$$\frac{N_A V s}{8p^2 e_r R^2}\left[\frac{2(1-\cos i)}{\sin^2 i}\right]^{1/2} \qquad (11)$$

For $e_q < i < 15$ degrees the factor involving inclination differs from unity by no more than 0.0086. Since the inclination of the inactive population of geosynchronous satellites typically does not exceed fifteen degrees [8], this factor may be taken equal to unity to obtain the collision rate as

$$\frac{N_A V s}{8p^2 e_r R^2} \qquad (12)$$

which is independent of inclination. Therefore, for N_I inactive objects with arbitrary inclination, but $e_q < i < 15$ individually, the collision rate is

$$\frac{N_I N_A V s}{8p^2 e_r R^2} \qquad (13)$$

The historical LSSC database can be used to determine the number of active and inactive satellites, N_A and N_I, deployed to geostationary orbit. However, although the database contains the launch year of an object, it does not contain the year the satellite went out of service. However, by assuming an equivalent, average satellite life and verifying that the estimate of the current population, which results using this equivalent, average life agrees with the actual current population, an estimate can be made of the active and inactive satellite population over time. Then, assuming e_r = 130 km so that the simplified result derived here agree with Hechler and Van der Ha, this approach gives an annual collision rate of 2.0×10^{-4} for the present population. Furthermore, this estimate indicates that the probability of collision has increased by an order of magnitude in about eleven years, although the rate of increase is slowing slightly, as shown in Fig. 6.

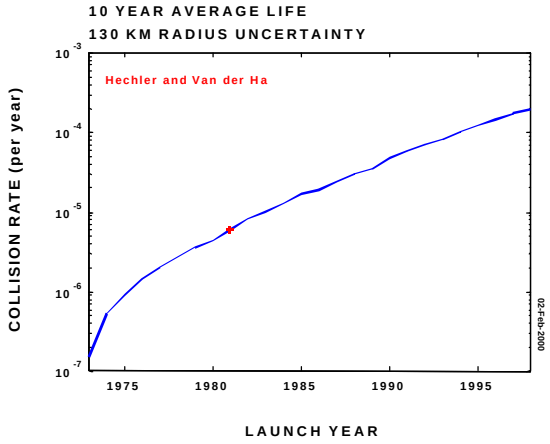

Fig. 6. Historical Collision Rate Growth

2.3 Probability of Collision based on Station Keeping Behavior

Active satellites in the geostationary orbit occupy a well-defined location by regulation and operational procedure. The International Telecommunication Union, publisher of the Radio Regulations (in effect, an international treaty), coordinates frequency and longitude assignments for geostationary communication satellites. Satellite operators typically control the longitude and inclination within ±0.05 degrees in order to comply with this regulation. Operators perform longitude control maneuvers, termed east-west station keeping maneuvers, every two weeks, typically. Such maneuvers are required due to the geopotential of the earth, which tends to accelerate the satellite toward a geopotential well.

Since inactive satellites typically orbit appreciably inclined to the equator, they encounter the active, station-kept satellites with a relative velocity approximately perpendicular to the equatorial plane. Therefore, it is instructive to consider the position of the active satellites in an earth centered, fixed coordinate system XYZ where Z aligns with the earth's axis of rotation and X passes through the Greenwich meridian. Consider, for example, a typical partner satellite which will be termed PartnerSat 1. A recent element set may be propagated for two weeks in order to represent the motion of the satellite over an east-west station keeping cycle. By collecting the same result for, say, nine additional recent but different element sets, a statistically

representative sample for the PartnerSat 1 east-west station-keeping performance is obtained.

Such a process is illustrated in Figs. 7 and 8. Fig. 7 shows the longitude over ten 14-day segments, which result from the selected element sets. Fig. 8 shows, in red, the orbit of PartnerSat 1 over one day for one particular element set, in yellow, the orbit for the same element set over the remaining 13 days and, in cyan, the orbit over 14 days of the remaining element sets. Note that although some of the element sets exhibit the expected station-keeping behavior expected, others exhibit an elevated drift rate. Nevertheless, the following results will demonstrate that the distribution of position is very adequately represented for the purpose of calculating the probability of collision.

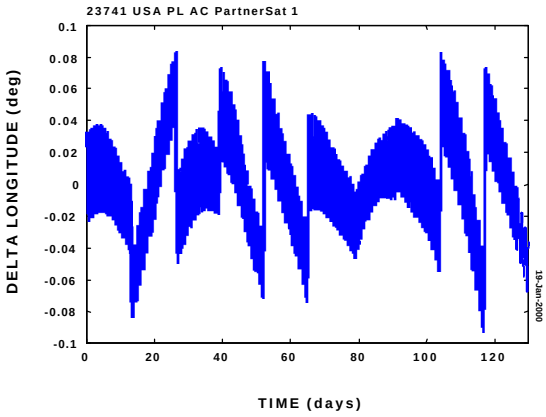

Fig. 7. Longitude Behavior for Ten Representative Station Keeping Periods

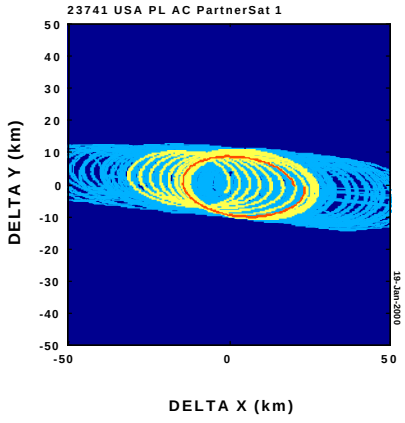

Fig. 8. Relative Position During Ten Representative Station Keeping Periods

During an encounter in which an inactive object occupies some region of the *XY* plane at the same time in which PartnerSat 1 occupies the same region, a collision is possible. The probability of a collision is given by the fraction of time PartnerSat 1 spends in this portion of the *XY* plane multiplied by the ratio of the collision area to the resolution cell area, as discussed above. Note that the size of the resolution cell must be chosen such that the maximum velocity of PartnerSat 1, relative to the center of its station-keeping box, does not cause the position of the satellite to step over a resolution cell during one propagation step. The resulting probability of collision distribution for PartnerSat 1 is shown in Fig. 9. Note that the size of the station-keeping box was taken to be 100 km on a side, which accounts for 96.9% of the propagated positions and that a collision radius of 50 m was assumed.

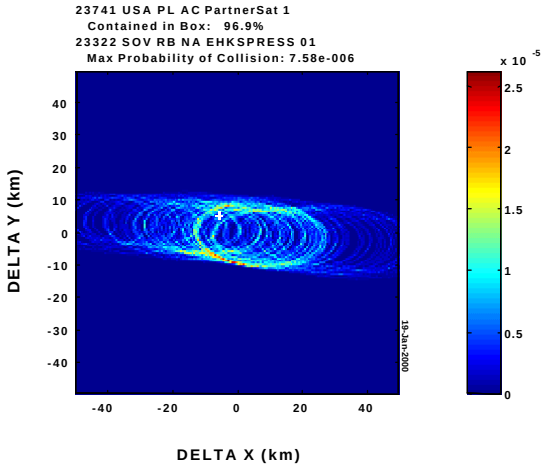

Fig. 9. Typical Probability of Collision Distribution

As mentioned above, the set of threat objects may be reliably propagated with DYNAMO over even long spans. DYNAMO is a general-purpose orbit determination and ephemeris generation program based on strictly numerical methods to solve the equations of motion. DYNAMO uses the JGM3 gravity field model, includes direct lunar and solar effects, models body tides, solar radiation pressure, earth-reflected radiation and atmospheric drag, and simulates thrust forces and is capable of generating one-meter orbits given suitable observations. For the result presented here, the inactive objects are propagated over a one-year time period spanning approximately October 1999 to October 2000. The positions are compared to the position of each active object to determine the occurrences of an encounter, defined as a difference in position in the *XY* plane of no more than 50 km and in the *Z* direction of no more than 125 km. Note that an interpolation is done of the propagated position to times separated by no more than the time required for an inactive, geosynchronous object to travel 250 km in the *Z* direction by noting again that the maximum inclination of an inactive, geosynchronous satellite is fifteen degrees [8].

the corresponding relative velocity used to transform the *XY* plane into one normal to this relative velocity. Unique encounters are determined as before, although in the transformed coordinates. An encounter is considered unique if it occurs no more frequently than a quarter orbital period. The white plus in Fig. 9 shows the position at which a Russian rocket body for Ehkspress I encounters PartnerSat 1 and the corresponding probability of collision. Note that assuming a uniform distribution of the active satellite over a 100 km square and a 50 m collision radius would give a probability of collision of 7.9×10^{-7}. Therefore the result for this particular encounter between PartnerSat 1 and Ehkspress I has a probability of collision which is nearly an order of magnitude larger. An additional case involving Telstar 401 is shown in Fig. 10.

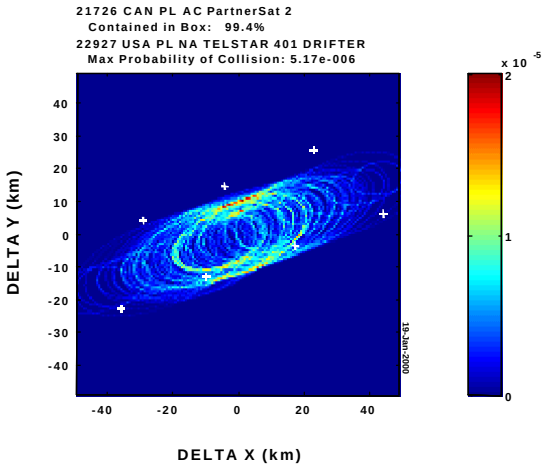

Fig. 10. Typical Encounter with Telstar 401

Following this same approach, the probability of collision for every encounter occurring between the entire population of active, geostationary satellites and all inactive objects capable of reaching the geosynchronous altitude can be determined. A histogram describing the resulting distribution of probability of collision may be calculated, each value of which may be multiplied by the probability of collision value for each bin to obtain the distribution shown in Fig. 11. The result shows the contribution to the total probability of collision for each bin and therefore that the total probability of collision is not dominated by large outliers. Overall, the results indicate that the annual probability of collision for the entire threat source population against the entire active population is 4.1×10^{-3}. As a sanity check, note that the total number of encounters corresponding to this result is 4364 which, when multiplied by the probability of collision corresponding to a uniform distribution (7.9×10^{-7}), gives an annual probability of collision equal to 3.4×10^{-3}.

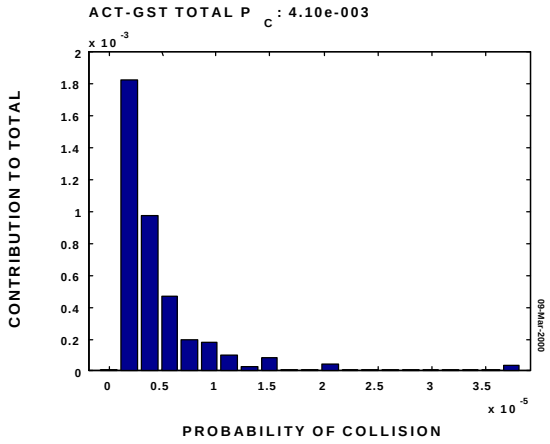

Fig. 11. Probability of Collision Contributions

3. CONCLUSIONS

The probability of collision between the population of active, geostationary satellites and inactive, geosynchronous objects has been reliably characterized. A new approach based on active satellite east-west station keeping performance has been presented and compared with previously published approaches based on volume density or orbital covariances. The approaches have been shown to be conceptually consistent and provide order of magnitude quantitative agreement. The new results indicate that, today, the annual probability of collision is more than one in one thousand, a result significantly larger than a previous, less detailed, volume density based estimate.

The probability of collision in the geostationary orbit, small but not negligible, inevitably results from the technological development and historical operation of geostationary satellite communications. Although unfortunate, the failure of Telstar 401 has provided the motivation and resources, through the cooperative agreement between MIT Lincoln Laboratory and commercial satellite operators, to understand and begin responding to this orbital situation. Lincoln Laboratory now posses a validated concept of operations for providing encounter support, procedures for routinely calibrating transponder ranging data and approaches for maximizing orbital precision while minimizing sensor time requirements. Under a continuing cooperative agreement, Lincoln Laboratory will use these results to develop a system for monitoring encounters between all cataloged threatening resident space objects and partner satellites to provide the technology to confidently and efficiently address the geosynchronous encounter situation now and in the future.

4. REFERENCES

1. R.I. Abbot, L.E. Thornton, and D.E. Whited, "Close Encounter Analyses of Telstar 401 with Satellites in the Geopotential Well 97-113 Degrees West longitude," Project Report CESA-1, May 1998, MIT Lincoln Laboratory.

2. R.I. Abbot and L.E. Thornton, "GEA CRDA Range Data Analysis," Project Report CESA-2, March 1999, MIT Lincoln Laboratory.

3. R. I. Abbot and J. Sharma, "Determination of Accurate Orbits for Close Encounters between Geosynchronous Satellites," Proceedings of the 1999 Space Control Conference, Lexington, Massachusetts, 13-15 April 1999, MIT Project Report STK-254, 71-85.

4. M. Hechler and J.C. Van der Ha, "Probability of Collisions in the Geostationary Ring," *J. Spacecraft*, 18(4), 361-366, July-August 1981.

5. D.J. Kessler, "Derivation of the Collision Probability between Orbiting Objects: The Lifetimes of Jupiter's Outer Moons," *Icarus* 48, 39-48, 1981.

6. K. T. Alfriend, M. R. Akella, D-J. Lee, J. Frisbee, and J. L. Foster, "Probability of Collision Error Analysis," *Proceedings of the 1998 AIAA/AAS Astrodynamics Specialist Conference*, Boston, Massachusetts, 10-12 August 1998.

7. K. Chan, "Collision Probability Analyses for Earth Orbiting Satellites," *Advances in the Astronautical Sciences* 96, 1033-1048, 1997.

8. L.J. Friesen, A.A. Jackson, IV, H.A. Zook, and D.J. Kessler, "Analysis of Orbital Perturbations Acting on Objects in Orbits Near Geosynchronous Earth Orbit," *J. of Geophysical Research*, 97(E3), 3845-3863, 25 March 1992.